Molecular Cell, Volume *74*

Supplemental Information

Analysis of the Human Kinome and Phosphatome by Mass Cytometry Reveals Overexpression-Induced Effects on Cancer-Related Signaling

Xiao-Kang Lun, Damian Szklarczyk, Attila Gábor, Nadine Dobberstein, Vito Riccardo Tomaso Zanotelli, Julio Saez-Rodriguez, Christian von Mering, and Bernd Bodenmiller

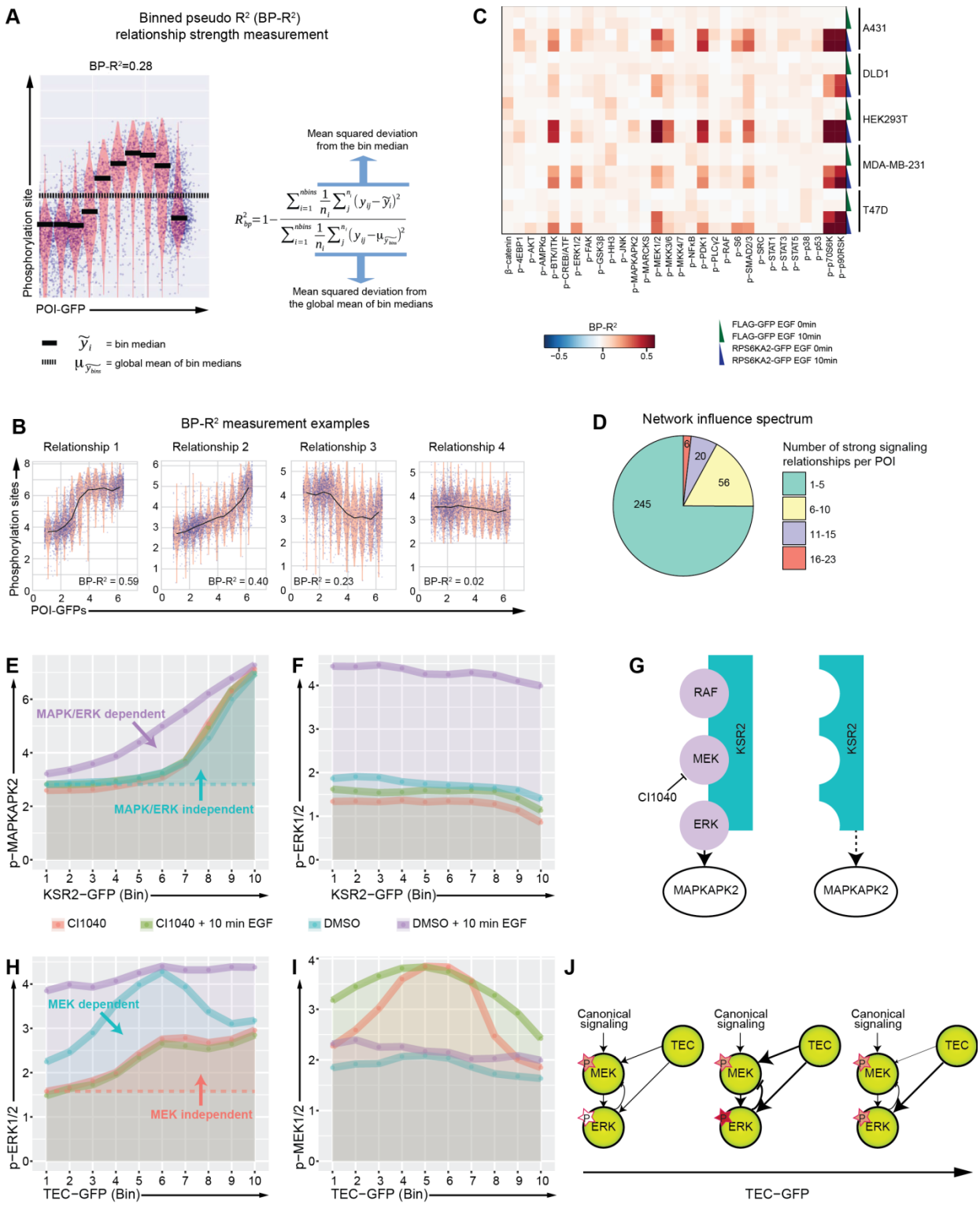

Figure S1. Kinase and phosphatase overexpression impacts cell signaling, Related to Figure 1

A, BP-R^2 is a density-independent analysis that measures protein abundance-dependent signaling relationship strength by quantifying deviation from bin median versus the global mean of bin medians (Lun et al., 2017). **B**, BP-R^2 analysis is robust in measuring the strength of complex signaling relationships regardless of their directionality, linearity, and average signal levels. **C**, Heat map of signaling relationship strength (as quantified by BP-R^2) between overexpressed RPS6KA2-GFP or the control FLAG-GFP to every measured phosphorylation site with or without 10-minute EGF stimulation. Signaling relationships assessed with HEK293T cells were reproducible in four other cell lines from different origins, including a epidermoid carcinoma cell line A431, a colorectal adenocarcinoma cell line DLD1, a breast adenocarcinoma cell line MDA-MB-231, and a breast ductal carcinoma cell line T47D. **D**, Pie chart shows the number of POIs that have strong (BP-R^2 > 0.13) overexpression-induced signaling relationships to the measured phosphorylation sites. Three-fourths of the POIs modulated one to five phosphorylation sites. **E-F,** Signaling relationships between KSR2-GFP to p-MAPKAPK2 (Thr334) or to p-ERK1/2 (Thr202/Tyr204) with four different treatments indicated with line colors. KSR2 overexpression caused an exponential increase in phosphorylation levels of MAPKAPK2 in the absence of EGF. Upon EGF stimulation, this relationship became linear. MEK inhibitor CI1040 did not influence the KSR2 overexpression-dependent MAPKAPK2 phosphorylation, although it drastically reduced the p-ERK1/2 levels, suggesting a MAPK/ERK-independent MAPKAPK2 activation pathway that is turned on only when KSR2 is present at high levels. **G,** KSR2 abundance-dependent p-MAPKAPK2 signaling can be MAPK/ERK cascade-dependent (left) or MAPK/ERK cascade-independent (right). **H-J,** Signaling relationships between TEC-GFP and p-ERK1/2 or between TEC-GFP and p-MEK1/2 with four different treatments indicated with line colors. Increased TEC abundance led to non-monotonic ERK1/2 phosphorylation that could be partially diminished by MEK inhibition, indicating the presence of both MEK-dependent and MEK-independent pathways for the TEC overexpression-induced ERK activation. CI1040 inhibited MEK activity and its dephosphorylating processes (Allen et al., 2003). Thus, the bow-like TEC to p-MEK1/2 relationship shape under the CI1040 treatment condition indicated the reduction of signal input to MEK at high TEC expression levels.

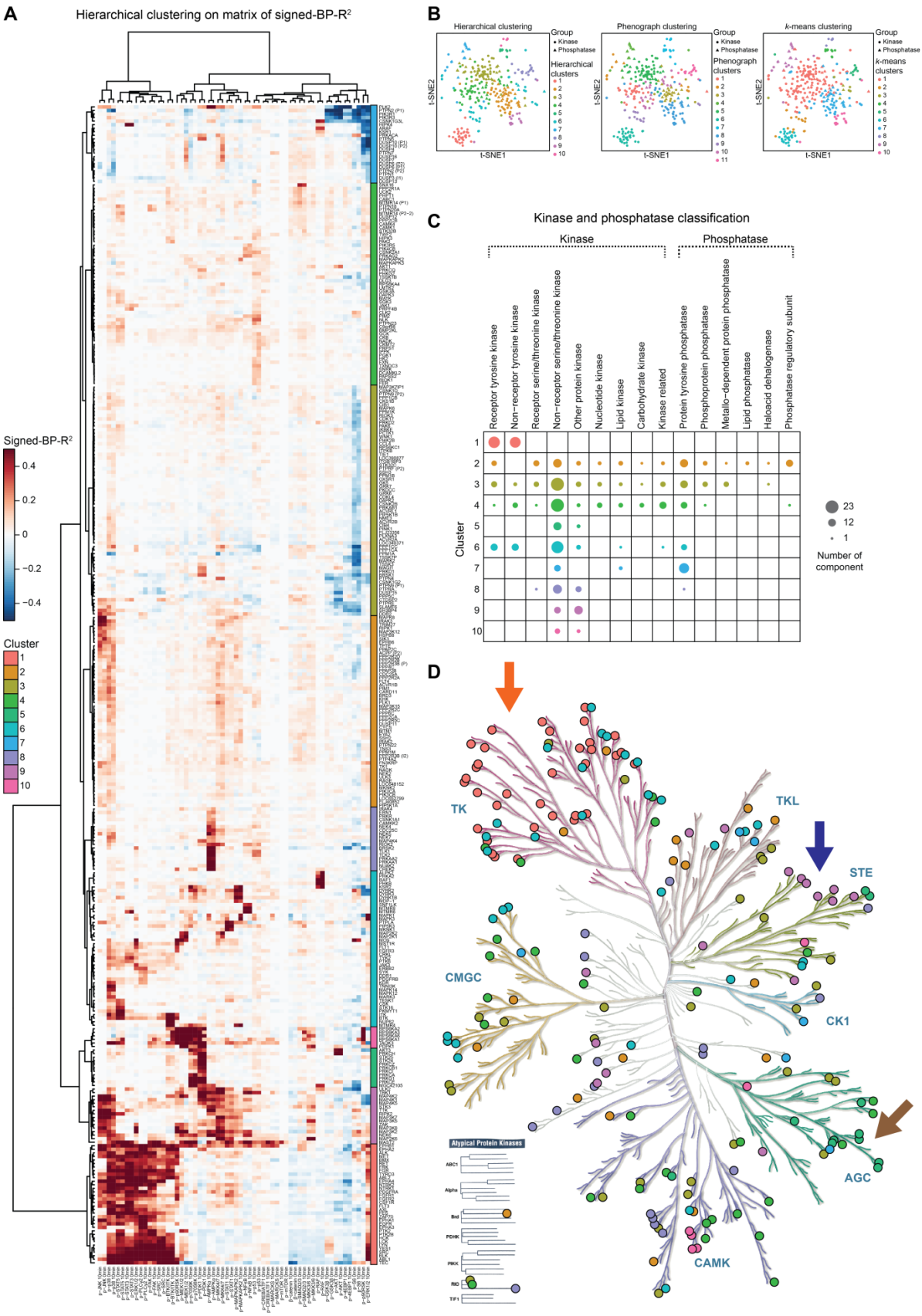
A
Hierarchical clustering on matrix of signed-BP-R²
Signed-BP-R²
0.4
0.2
0
−0.2
−0.4
Cluster
1
2
3
4
5
6
7
8
9
10
B
Hierarchical clustering
Phenograph clustering
k-means clustering
Group
Kinase
Phosphatase
Hierarchical clusters
Phenograph clusters
k-means clusters
t-SNE1
t-SNE2
C
Kinase and phosphatase classification
Kinase
Phosphatase
Receptor tyrosine kinase
Non−receptor tyrosine kinase
Receptor serine/threonine kinase
Non−receptor serine/threonine kinase
Other protein kinase
Nucleotide kinase
Lipid kinase
Carbohydrate kinase
Kinase related
Protein tyrosine phosphatase
Phosphoprotein phosphatase
Metallo−dependent protein phosphatase
Lipid phosphatase
Haloacid dehalogenase
Phosphatase regulatory subunit
Cluster
Number of component
23
12
1
D
TK
TKL
STE
CMGC
CK1
AGC
CAMK
Atypical Protein Kinases
ABC1
Alpha
Bnd
PDHK
PIKK
RIO
TIF1

Figure S2. Classification of kinases and phosphatases based on abundance-dependent effects to cancer signaling networks, Related to Figure 2

A, Heat map shows the signed-BP-R^2 of all 327 cancer signaling network-influencing POIs (i.e., POIs with at least one strong overexpression-induced signaling relationship, BP-R^2 > 0.13) to every phosphorylation site with or without 10-minute EGF stimulation. Hierarchical clustering identified 10 groups of kinases or phosphatases with the similar network-influencing properties. **B**, Three different clustering methods, hierarchical clustering, Phenograph (Levine et al., 2015), and *k*-means clustering show similar results on kinase and phosphatase overexpression effects, as color-coded on t-SNE plots. **C**, Corresponding components between identified hierarchical clusters (the same cluster color code as in panel **(A)**, and kinase/phosphatase classifications based on the sequence of protein catalytic domains. **D**, Kinases with strong network effects plotted on the phylogenetic tree of the human kinome, with the clusters number assigned in panel **(A)** as color-code (Illustration reproduced courtesy of Cell Signaling Technology, Inc. www.cellsignal.com).

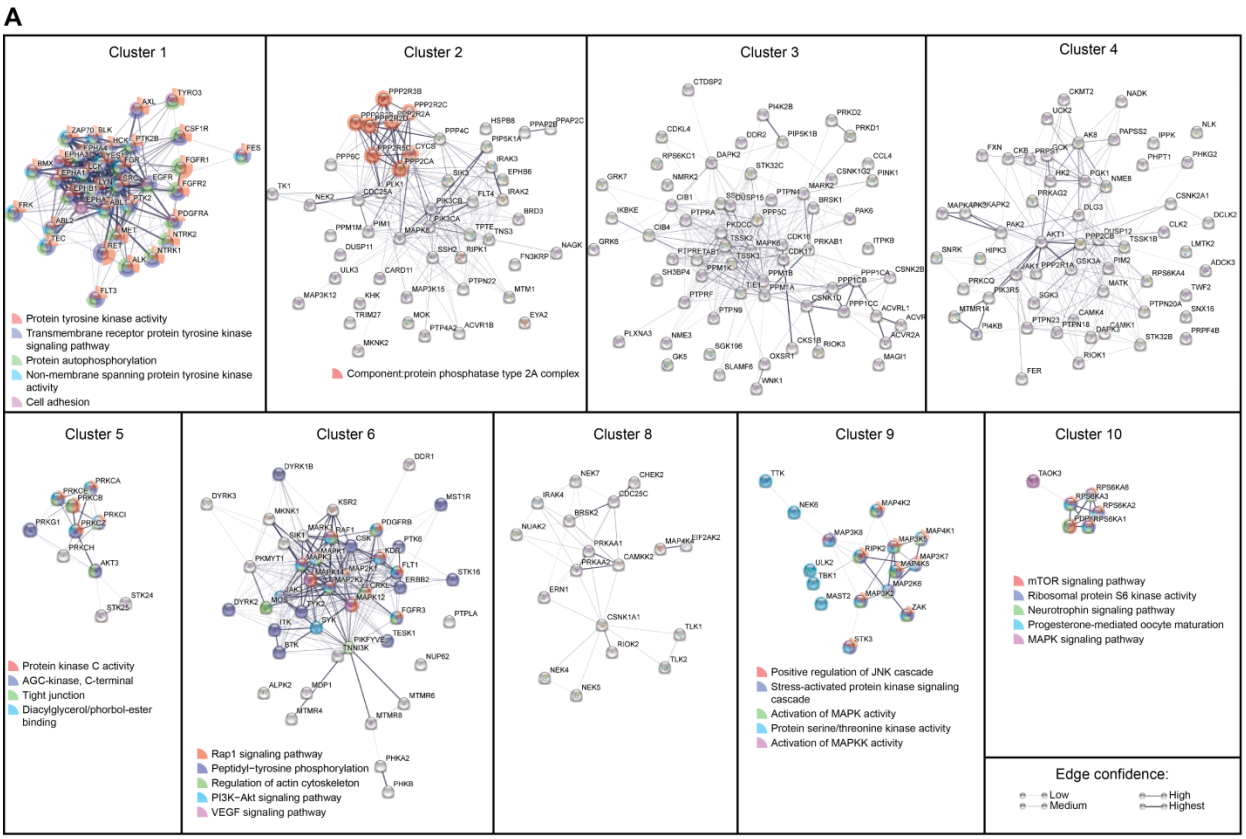

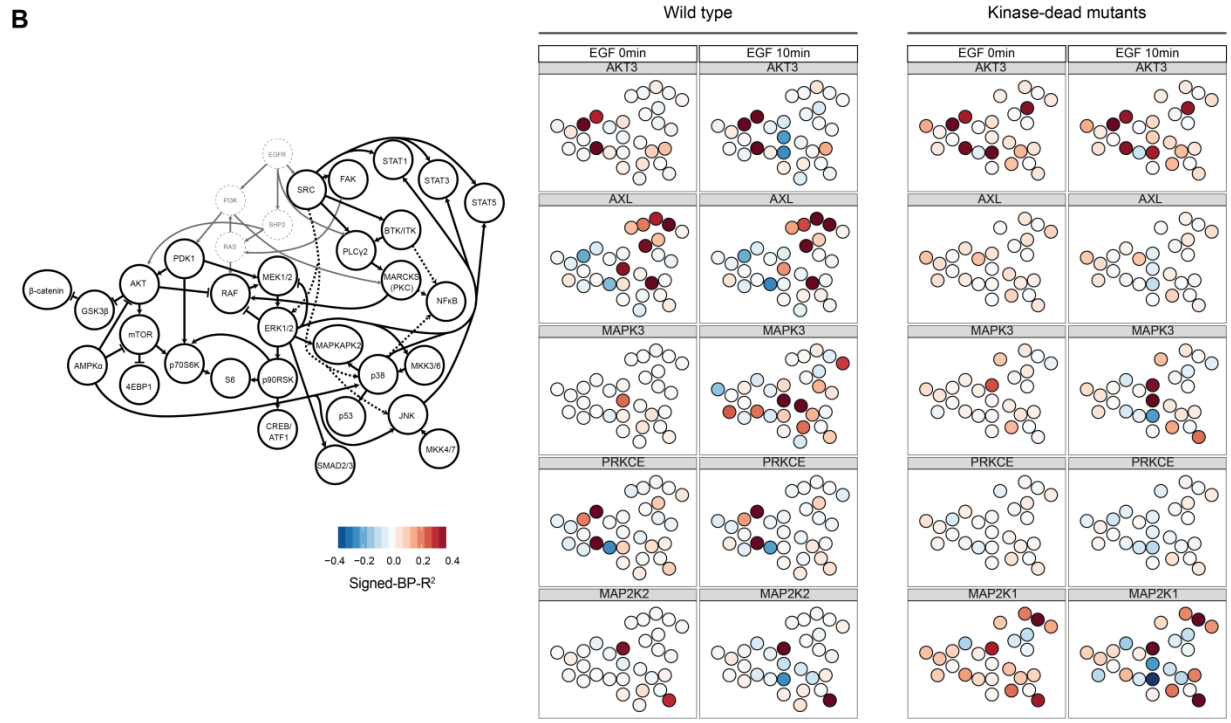

Figure S3. Comparison of kinase and phosphatase overexpression effects to their catalytic functions, Related to Figure 3

A, Functional association analysis was performed for clusters 1, 2, 3, 4, 5, 6, 8, 9, and 10. Edges with confidence above 0.2 are shown in the network. Functional enrichments are color-coded and labeled on the nodes. **B**, Analysis of wild-type kinases AKT3, AXL, MAPK3, PRKCE, MAP2K2, and kinase-dead mutants $AKT3^{K177M}$, AXL^{K567R}, $MAPK3^{K71R}$, $PRKCE^{K437W}$, and $MAP2K1^{K97M}$ on abundance-dependent effects to the signaling network with and without 10 min EGF stimulation.

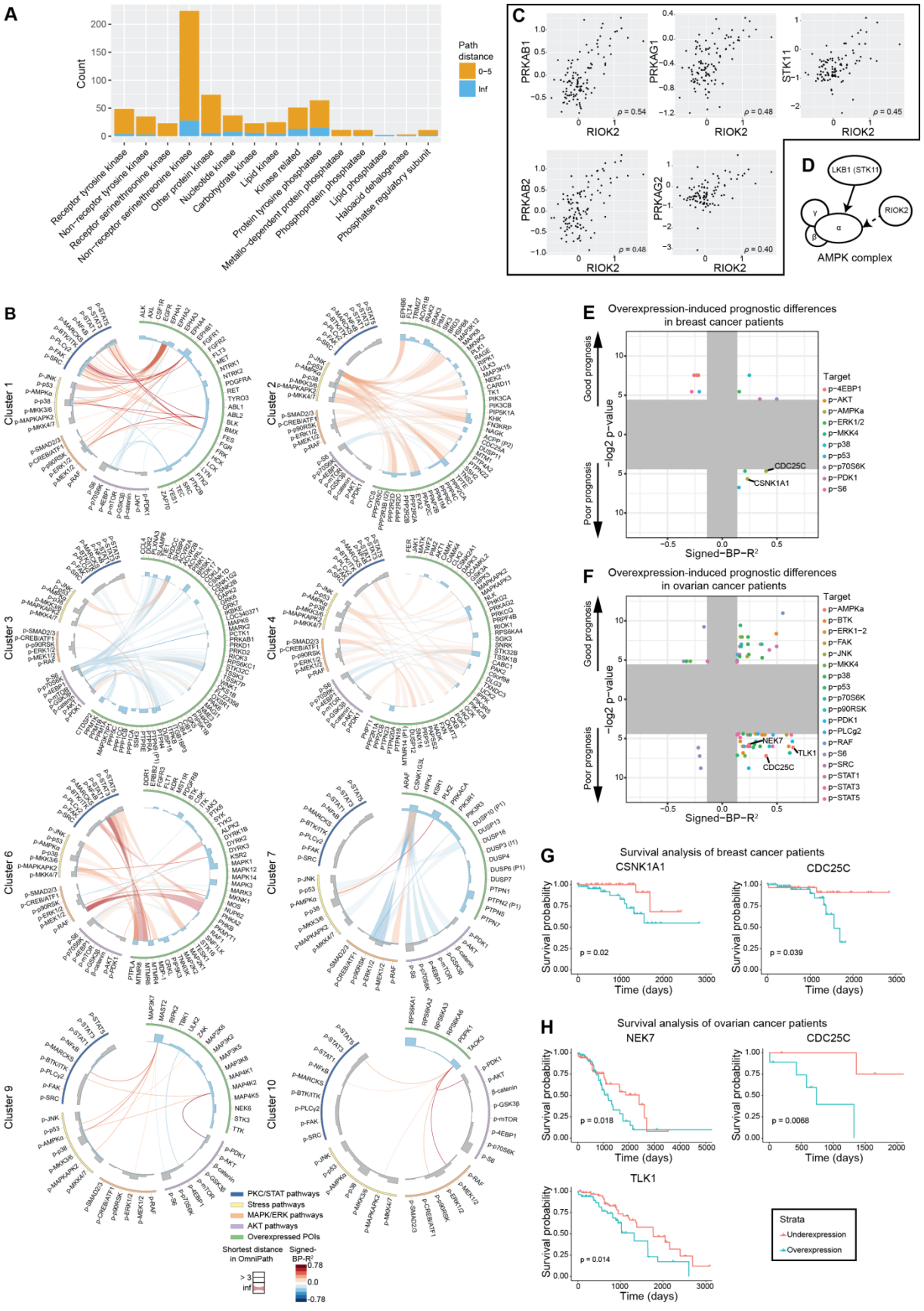
A
Count
Path distance
0–5
Inf
Receptor tyrosine kinase
Non−receptor tyrosine kinase
Receptor serine/threonine kinase
Non−receptor serine/threonine kinase
Other protein kinase
Nucleotide kinase
Carbohydrate kinase
Lipid kinase
Kinase related
Protein tyrosine phosphatase
Metallo−dependent protein phosphatase
Phosphoprotein phosphatase
Lipid phosphatase
Haloacid dehalogenase
Phosphatase regulatory subunit
C
PRKAB1
PRKAG1
STK11
PRKAB2
PRKAG2
RIOK2
D
LKB1 (STK11)
RIOK2
AMPK complex
B
Cluster 1
Cluster 2
Cluster 3
Cluster 4
Cluster 6
Cluster 7
Cluster 9
Cluster 10
PKC/STAT pathways
Stress pathways
MAPK/ERK pathways
AKT pathways
Overexpressed POIs
Shortest distance in OmniPath
Signed-BP-R²
E
Overexpression-induced prognostic differences in breast cancer patients
Good prognosis
Poor prognosis
−log2 p−value
Signed−BP−R²
Target
CDC25C
CSNK1A1
F
Overexpression-induced prognostic differences in ovarian cancer patients
NEK7
TLK1
CDC25C
G
Survival analysis of breast cancer patients
CSNK1A1
CDC25C
Survival probability
Time (days)
p = 0.02
p = 0.039
H
Survival analysis of ovarian cancer patients
NEK7
CDC25C
TLK1
p = 0.018
p = 0.0068
p = 0.014
Strata
Underexpression
Overexpression

Figure S4. Potential signaling relationships detected by the kinome and phosphatome screen reveal overexpression-induced AMPK activation is related to poor prognosis in cancer patients, Related to Figure 4

A, Counts of strong (BP-R^2 > 0.13) abundance-dependent signaling relationships with shortest signed directed path length of 0-5 or with infinite path length (calculated using the Omnipath database) for each sequenced-based kinase and phosphatase classification. **B**, Shortest signed directed path length for each identified signaling relationships shown in Circos plots for the clusters of 1, 2, 3, 4, 6, 7, 9, and 10. **C**, CPTAC proteome study on TCGA breast invasive carcinoma samples (Koboldt et al., 2012) shows highly correlated expression levels between RIOK2 and AMPK subunit β (PRKAB1, PRKAB2), γ (PRKAG1, PRKAG2), and AMPK upstream regulator LKB1 (STK11). **D**, Model of the AMPK complex. AMPK activity can be controlled by an upstream kinase LKB1 (STK11) and by RIOK2. **E-F**, The relevance of kinase and phosphatase overexpression and the prognosis of breast cancer **(E)** and ovarian cancer **(F)** patients were assessed, and plotted against abundance-dependent signaling relationship strengths quantified by signed-BP-R^2. Kinases with capability for overexpression-induced AMPK activation (annotated on the plots) were found to be associated with significantly worse patient prognosis in both cancer types. **G-H**, Survival analysis of breast cancer patients with CSNK1A1 or CDC25C overexpression, and ovarian cancer patients with NEK7, TLK1, or CDC25C overexpression.

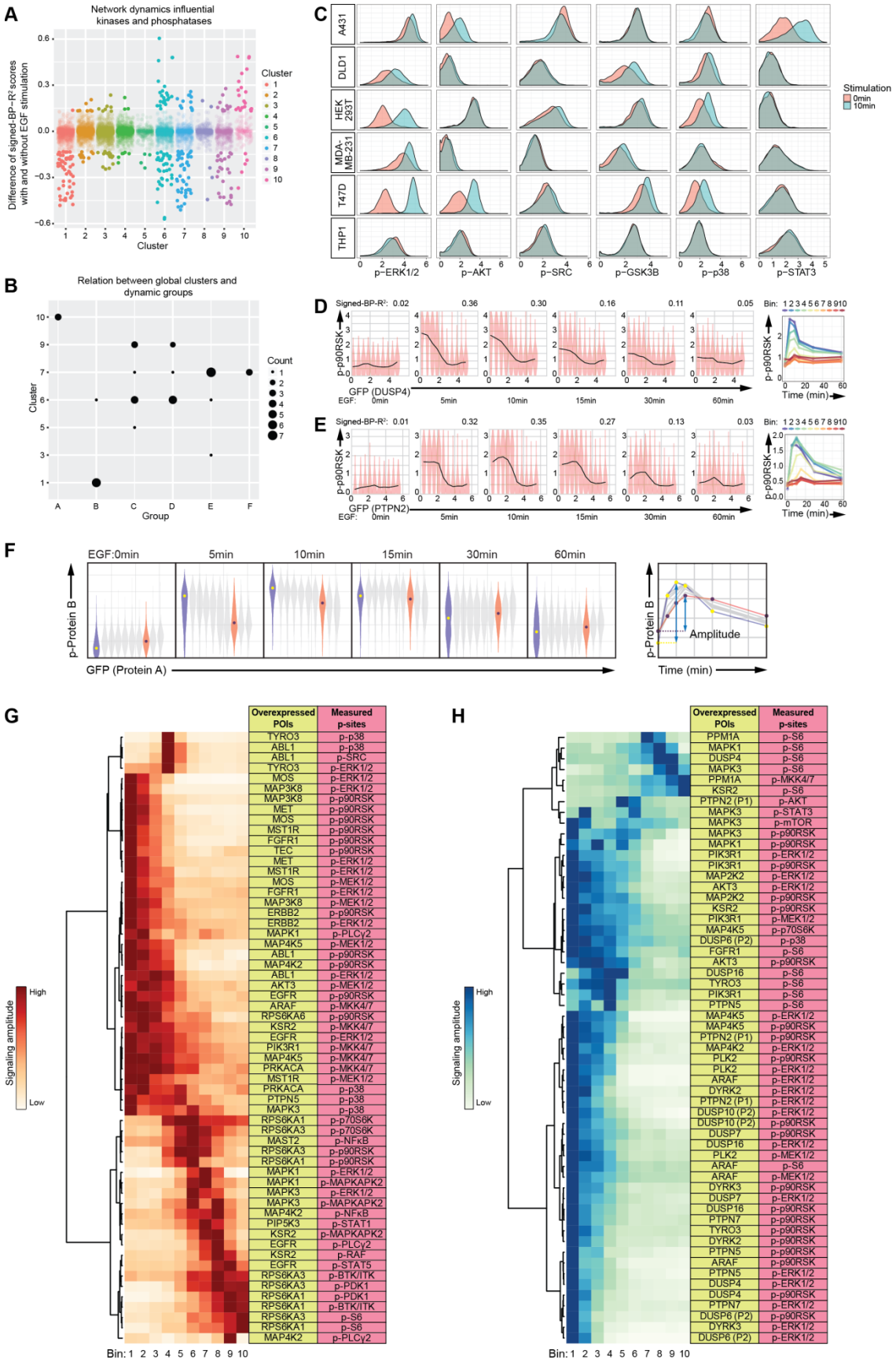
A
Network dynamics influential kinases and phosphatases
Difference of signed-BP−R² scores with and without EGF stimulation
Cluster
B
Relation between global clusters and dynamic groups
Cluster
Group
Count
C
A431
DLD1
HEK 293T
MDA-MB-231
T47D
THP1
p−ERK1/2
p−AKT
p−SRC
p−GSK3B
p−p38
p−STAT3
Stimulation
0min
10min
D
Signed-BP-R²: 0.02 0.36 0.30 0.16 0.11 0.05
p-p90RSK
GFP (DUSP4)
EGF: 0min 5min 10min 15min 30min 60min
Bin: 1 2 3 4 5 6 7 8 9 10
Time (min)
E
Signed-BP-R²: 0.01 0.32 0.35 0.27 0.13 0.03
GFP (PTPN2)
F
EGF:0min 5min 10min 15min 30min 60min
p-Protein B
GFP (Protein A)
Amplitude
Time (min)
G
Overexpressed POIs
Measured p-sites
TYRO3 p-p38
ABL1 p-p38
ABL1 p-SRC
TYRO3 p-ERK1/2
MOS p-ERK1/2
MAP3K8 p-ERK1/2
MAP3K8 p-p90RSK
MET p-p90RSK
MOS p-p90RSK
MST1R p-p90RSK
FGFR1 p-p90RSK
TEC p-p90RSK
MET p-ERK1/2
MST1R p-ERK1/2
MOS p-MEK1/2
FGFR1 p-ERK1/2
MAP3K8 p-MEK1/2
ERBB2 p-p90RSK
ERBB2 p-ERK1/2
MAPK1 p-PLCγ2
MAP4K5 p-MEK1/2
ABL1 p-p90RSK
MAP4K2 p-p90RSK
ABL1 p-ERK1/2
AKT3 p-MEK1/2
EGFR p-p90RSK
ARAF p-MKK4/7
RPS6KA6 p-p90RSK
KSR2 p-MKK4/7
EGFR p-ERK1/2
PIK3R1 p-MKK4/7
MAP4K5 p-MKK4/7
PRKACA p-MKK4/7
MST1R p-MEK1/2
PRKACA p-p38
PTPN5 p-p38
MAPK3 p-p38
RPS6KA1 p-p70S6K
RPS6KA3 p-p70S6K
MAST2 p-NFκB
RPS6KA3 p-p90RSK
RPS6KA1 p-p90RSK
MAPK1 p-ERK1/2
MAPK1 p-MAPKAPK2
MAPK3 p-ERK1/2
MAPK3 p-MAPKAPK2
MAP4K2 p-NFκB
PIP5K3 p-STAT1
KSR2 p-MAPKAPK2
EGFR p-PLCγ2
KSR2 p-RAF
EGFR p-STAT5
RPS6KA3 p-BTK/ITK
RPS6KA3 p-PDK1
RPS6KA1 p-PDK1
RPS6KA1 p-BTK/ITK
RPS6KA3 p-S6
RPS6KA1 p-S6
MAP4K2 p-PLCγ2
Signaling amplitude
High
Low
Bin: 1 2 3 4 5 6 7 8 9 10
H
Overexpressed POIs
Measured p-sites
PPM1A p-S6
MAPK1 p-S6
DUSP4 p-S6
MAPK3 p-S6
PPM1A p-MKK4/7
KSR2 p-S6
PTPN2 (P1) p-AKT
MAPK3 p-STAT3
MAPK3 p-mTOR
MAPK3 p-p90RSK
MAPK1 p-p90RSK
PIK3R1 p-ERK1/2
PIK3R1 p-p90RSK
MAP2K2 p-ERK1/2
AKT3 p-ERK1/2
MAP2K2 p-p90RSK
KSR2 p-p90RSK
PIK3R1 p-MEK1/2
MAP4K5 p-p70S6K
DUSP6 (P2) p-p38
FGFR1 p-S6
AKT3 p-p90RSK
DUSP16 p-S6
TYRO3 p-S6
PIK3R1 p-S6
PTPN5 p-S6
MAP4K5 p-ERK1/2
MAP4K5 p-p90RSK
PTPN2 (P1) p-p90RSK
MAP4K2 p-ERK1/2
PLK2 p-p90RSK
PLK2 p-ERK1/2
ARAF p-ERK1/2
DYRK2 p-ERK1/2
PTPN2 (P1) p-ERK1/2
DUSP10 (P2) p-ERK1/2
DUSP10 (P2) p-p90RSK
DUSP7 p-p90RSK
DUSP16 p-ERK1/2
PLK2 p-MEK1/2
ARAF p-S6
ARAF p-MEK1/2
DYRK3 p-p90RSK
DUSP7 p-ERK1/2
DUSP16 p-p90RSK
PTPN7 p-p90RSK
TYRO3 p-p90RSK
DYRK2 p-p90RSK
PTPN5 p-p90RSK
ARAF p-p90RSK
PTPN5 p-ERK1/2
DUSP4 p-ERK1/2
DUSP4 p-p90RSK
PTPN7 p-ERK1/2
DUSP6 (P2) p-p90RSK
DYRK3 p-ERK1/2
DUSP6 (P2) p-ERK1/2
Signaling amplitude
High
Low
Bin: 1 2 3 4 5 6 7 8 9 10

Figure S5. Analysis of kinase and phosphatase overexpression-dependent signaling dynamics in EGF stimulation time course, Related to Figure 5

A, Variances of signed-BP-R^2 between cells with or without 10-minute EGF treatment are plotted for all identified clusters in the global analysis. **B**, Correspondence analysis shows to which 10 clusters as derived from the kinome and phosphatome analysis, the six dynamic signaling groups belong to. **C**, Phosphorylation levels of p-ERK1/2, p-AKT, p-SRC, p-GSK3β, p-p38, and p-STAT3 were assessed with and without 10-minute EGF stimulation in cell lines of A431, DLD1, HEK293T, MDA-MB-231, T47D, and THP1. **D-E**, Violin plots show cell distribution in each of ten bins based on GFP-tagged POI expression level for (**D**) DUSP4-GFP to p-p90RSK, and (**E**) PTPN2-GFP to p-p90RSK over the 1-hour EGF stimulation time course. Medians of all 10 bins are connected to indicate the shape of signaling relationships (black lines) with the relationship strength quantified by signed-BP-R^2, as shown on top of each individual plot. Medians of each bin over the 1-hour EGF stimulation time course are plotted separately to demonstrate the POI abundance-dependent signaling trajectories. **F**, Schematic plots of amplitude analysis. The abundance levels of the overexpressed GFP-POI were split into ten bins (left). Median phosphorylation in each bin over the 1-hour EGF stimulation time course are plotted to visualize abundance dependency of signaling amplitudes (right). **G-H**, Heat maps show pairs of signaling relationships with protein abundance-influenced signaling amplitudes with (**G**) positive relationships and (**H**) negative relationships determined by the summed Spearman correlation over all time points.

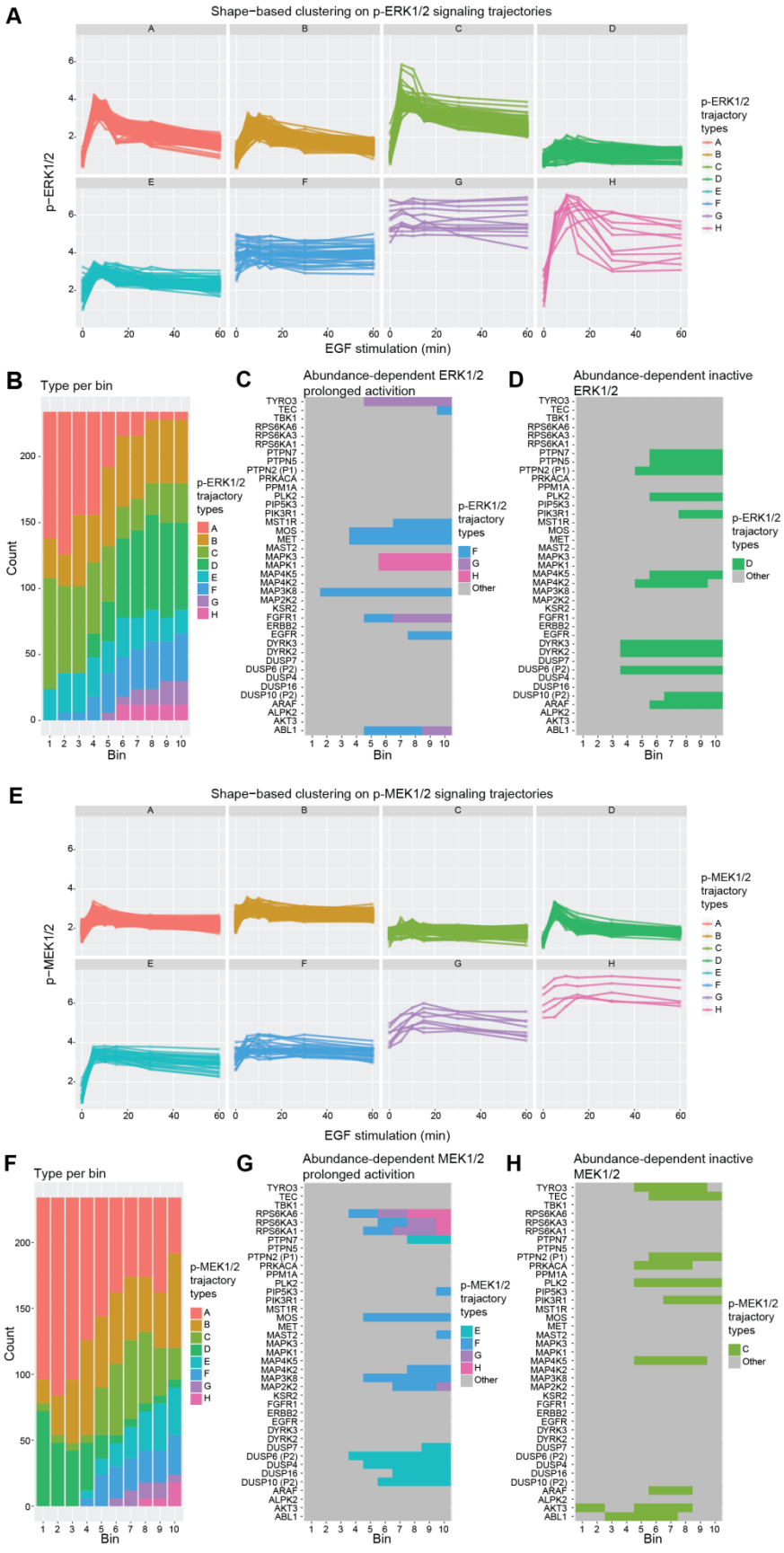
A
Shape−based clustering on p-ERK1/2 signaling trajectories
p−ERK1/2
EGF stimulation (min)
p-ERK1/2 trajectory types
B
Type per bin
Count
Bin
C
Abundance-dependent ERK1/2 prolonged activition
D
Abundance-dependent inactive ERK1/2
Other
E
Shape−based clustering on p-MEK1/2 signaling trajectories
p−MEK1/2
F
G
Abundance-dependent MEK1/2 prolonged activition
H
Abundance-dependent inactive MEK1/2

Figure S6. POI abundance-dependent p-ERK1/2 or p-MEK1/2 signaling trajectories, Related to Figure 5

A, Analyzing p-ERK1/2 signaling trajectories over the 1-hour EGF stimulation time course for each bin of the 39 assessed proteins using shape-based clustering (Genolini et al., 2015) resulted in the classification of eight trajectory types. **B**, Distributions of p-ERK1/2 trajectory types over the POI bins (expression levels) shows type D, F, G, and H only present with POI overexpression. **C**, The identification of kinases which cause abundance-dependent ERK1/2 prolonged activation. **D**, The identification of kinases and phosphatases that cause abundance-dependent ERK1/2 inactivation. **E**, Analyzing p-MEK1/2 signaling trajectories over the 1-hour EGF stimulation time course for each bin of the 39 assessed proteins using shape-based clustering resulted in the classification of eight trajectory types. **F**, Distributions of p-MEK1/2 trajectory types over the POI bins (expression levels) shows type E, F, G, and H only present with POI overexpression. **G**, The identification of kinases and phosphatases causing abundance-dependent MEK1/2 prolonged activation. **H**, Kinases and phosphatases that cause abundance-dependent MEK1/2 inactivation.

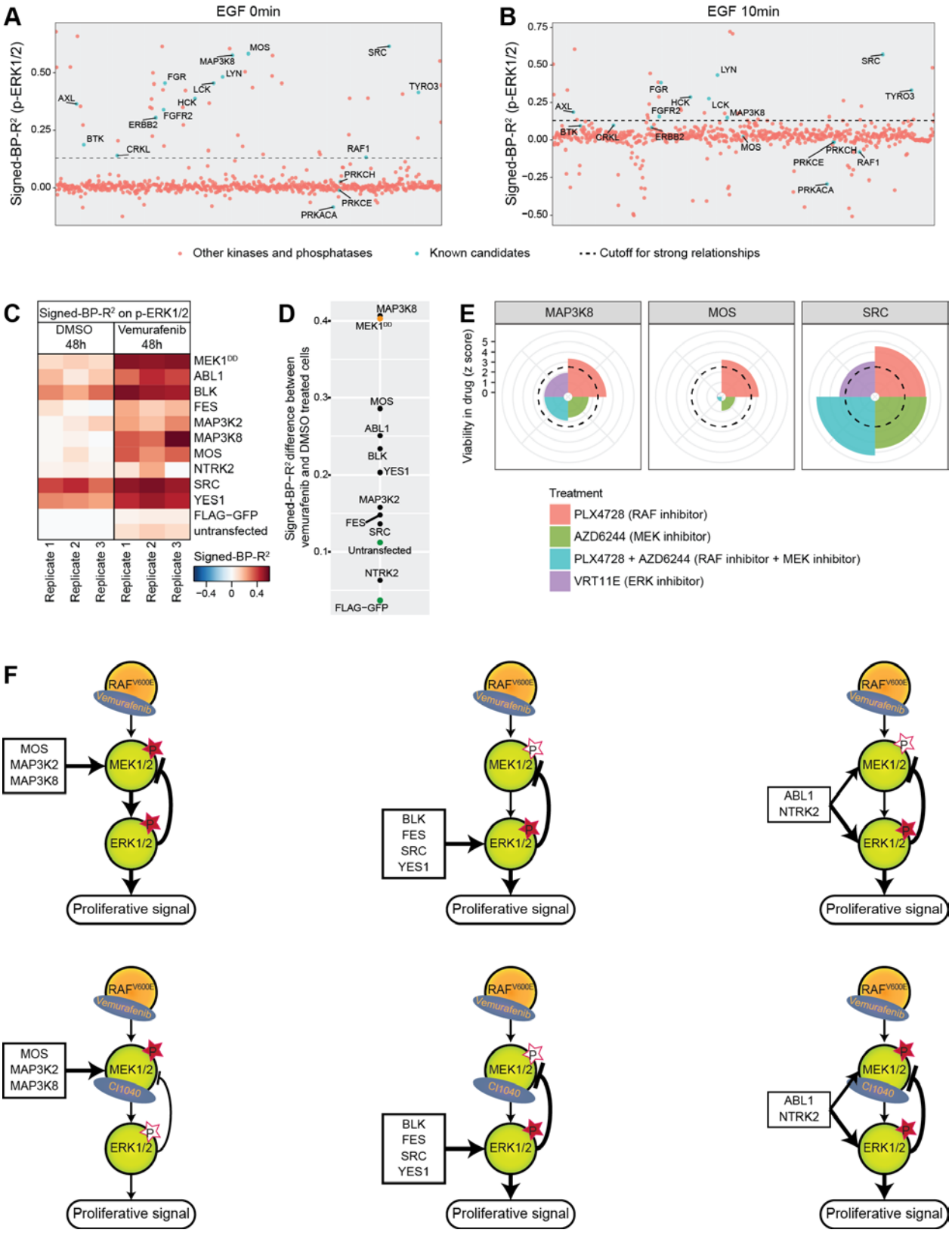
A
EGF 0min
Signed-BP-R² (p-ERK1/2)
B
EGF 10min
Other kinases and phosphatases
Known candidates
Cutoff for strong relationships
C
Signed-BP-R² on p-ERK1/2
DMSO 48h
Vemurafenib 48h
MEK1DD
ABL1
BLK
FES
MAP3K2
MAP3K8
MOS
NTRK2
SRC
YES1
FLAG−GFP
untransfected
Replicate 1
Replicate 2
Replicate 3
Signed-BP-R²
D
Signed-BP-R² difference between vemurafenib and DMSO treated cells
E
MAP3K8
MOS
SRC
Viability in drug (z score)
Treatment
PLX4728 (RAF inhibitor)
AZD6244 (MEK inhibitor)
PLX4728 + AZD6244 (RAF inhibitor + MEK inhibitor)
VRT11E (ERK inhibitor)
F
RAFV600E
Vemurafenib
MEK1/2
ERK1/2
Proliferative signal
MOS
MAP3K2
MAP3K8
BLK
FES
SRC
YES1
ABL1
NTRK2
CI1040

Figure S7. Kinase overexpression induces MAPK/ERK inhibition resistance in the melanoma A375 cell, Related to Figure 7

A-B, Signed-BP-R^2 values of each overexpressed POI to p-ERK1/2 (**A**) before and (**B**) after 10-minute EGF stimulation. Kinases previously shown to induce MAPK/ERK inhibition resistance in A375 cells (Johannessen et al., 2010, 2013) are labeled. 82.4% previously identified resistance-driving kinases can induce strong signaling relationship to p-ERK1/2 when overexpressed. **C**, Heat map of abundance-dependent relationship strength for each overexpressed POI to p-ERK1/2, quantified as signed-BP-R^2 from three replicate experiments. **D,** The mean differences of the three replicates between vemurafenib-treated cells and DMSO-treated cells in their signed-BP-R^2 scores with p-ERK1/2. **E**, Kinases of MAP3K8, MOS, and SRC were previously identified as candidates for MAPK/ERK inhibition resistance in A375 cells (Johannessen et al., 2013). Viability *z*-scores of A375 cells under four different inhibitor treatments are plotted using data from Johannessen et al., 2013. **F**, Models indicate the MAPK/ERK cascade states when cells overexpressing different MAPK/ERK reactivating kinases, under vemurafenib mono-treatment of vemurafenib-CI1040 combination.